Cardiorespiratory coupling in preterm infants

J Appl Physiol 126: 202–213, 2019.
First published November 1, 2018; doi:10.1152/japplphysiol.00722.2018.

RESEARCH ARTICLE

Cardiorespiratory coupling in preterm infants

Rohan Joshi,[1,2,3]* Deedee Kommers,[4,5]* Xi Long,[3] Loe Feijs,[1] Sabine Van Huffel,[6] Carola van Pul,[2,5] and Peter Andriessen[4]

[1]*Department of Industrial Design, Eindhoven University of Technology, Eindhoven, The Netherlands;* [2]*Department of Clinical Physics, Máxima Medical Centre, Veldhoven, The Netherlands;* [3]*Department of Fertility, Pregnancy and Parenting Solutions, Philips Research, Eindhoven, The Netherlands;* [4]*Department of Neonatology, Máxima Medical Centre, Veldhoven, The Netherlands;* [5]*Department of Applied Physics, Eindhoven University of Technology, Eindhoven, The Netherlands; and* [6]*KU Leuven, Department of Electrical Engineering, Division Stadius, and IMEC, Leuven, Belgium*

Submitted 16 August 2018; accepted in final form 29 October 2018

Joshi R, Kommers D, Long X, Feijs L, Van Huffel S, van Pul C, Andriessen P. Cardiorespiratory coupling in preterm infants. *J Appl Physiol* 126: 202–213, 2019. First published November 1, 2018; doi:10.1152/japplphysiol.00722.2018.—In preterm infants, a better understanding and quantification of cardiorespiratory coupling may help improve caregiving by enabling the tracking of maturational changes and subclinical signatures of disease. Therefore, in a study of 20 preterm infants admitted to a neonatal intensive care unit, we analyzed the cardiac and respiratory regulatory mechanisms as well as the coupling between them. In particular, we selectively analyzed coupling from changes in heart rate to respiratory oscillations as well as coupling from respiratory oscillations to the heart rate. Furthermore, we stratified this coupling based on decelerations and accelerations of the heart rate and by inspiration and expiration during respiration while contrasting periods of kangaroo care, an intervention known to enhance autonomic regulation, with periods in the incubator. We identified that preterm infants exhibit cardiorespiratory coupling that is nonsymmetric with regard to the direction of coupling. We demonstrate coupling from decelerations and accelerations of the heart rate to exhalation and inhalation, respectively, both on a beat-to-beat basis as well as with sustained decelerations and accelerations. On the other hand, on average, we also observed coupling from both inspiration and expiration to marginal decelerations in the heart rate. These phenomena, especially coupling from the changes in the heart rate to respiratory oscillations, were sensitive to whether the infant was receiving kangaroo care.

NEW & NOTEWORTHY Preterm infants exhibit cardiorespiratory coupling that is nonsymmetric with regard to the direction of coupling; coupling from fluctuations in the heart rate to respiratory oscillations and vice versa are asymmetric. On average, coupling is observable from decelerations or accelerations in the heart rate to inhalation or exhalation, respectively, whereas, on average, both peaks and troughs of respiration exhibit coupling to marginal decelerations in the heart rate.

autonomic regulation; cardiorespiratory coupling; kangaroo care; preterm infants; respiratory sinus arrhythmia

INTRODUCTION

Worldwide, 1 in 10 infants is born prematurely, and prematurity continues to remain the largest cause of neonatal morbidity and mortality (6). One of the causes of the increased vulnerability of preterm infants is an immature autonomic nervous system. In particular, the multiple feedback and control loops responsible for homeostasis are not yet fully developed and may not work synergistically (9). Notably, autonomic regulation in preterm infants is markedly different from that in term infants and adults (28, 32), precluding the possibility of directly translating physiological findings from these populations to preterm infants. A better understanding and quantification of autonomic regulation in preterm infants may help improve therapeutic practices by providing tools for tracking maturational changes and for detecting subclinical signatures of abnormal development (23).

When changes in autonomic regulation do not have a clear physiological explanation, as is often the case in the context of preterm infants, fundamental studies using experimental stimuli are required to elicit contrasting effects that can be interpreted from contextual information (1, 34). Often, such stimuli are experimentally designed stressors, the use of which is not possible in vulnerable preterm infants. Therefore, multiple studies have used periods of kangaroo care (KC) contrasted against periods in the incubator to study autonomic regulation in preterm infants (7, 15, 17, 19). KC is defined as an extended period of skin-to-skin contact, during which diaper-clad infants are held prone on the bare chest of one's parent. KC is widely accepted as comfortable and therapeutic and is proven to enhance autonomic regulation (8, 11).

Based on features of heart rate variability (HRV), previous research has demonstrated improved regulation during KC (19). During KC, HRV reduces owing to the reduced severity of heart rate decelerations, to which preterm infants are especially prone. The decrease in HRV during periods of increased comfort was a surprising finding since in adults lower HRV has been associated with poorer outcomes (38), highlighting again that commonly accepted physiological findings in adults may not be readily translated to preterm infants.

Similar to HRV-based measures of autonomic regulation, the respiratory dynamics of preterm infants also differ from that of adults (27). The respiratory dynamics exhibit immaturity due to underdeveloped chemoreceptors with abnormal responses to hypercarbia and hypoxia, leading to rapid, ineffi-

* R. Joshi and D. Kommers contributed equally and should be jointly considered first authors.

Address for reprint requests and other correspondence: Dept. of Industrial Design, Technical University of Eindhoven, PO Box 513, 5600 MB Eindhoven, The Netherlands (e-mail: r.joshi@tue.nl).

cient, and shallow breathing, including frequent cessations of breathing. In adults, the respiratory and cardiac systems can exhibit coupling, i.e., a preferential tendency, possibly synergistic, for the functioning of one system to be related to another (36). This phenomenon of cardiorespiratory coupling is challenging to quantify and has not frequently been studied in preterm infants. Although some studies have reported signs of cardiorespiratory coupling in preterm infants, patterns appeared different from the well-recognized coupling seen in adults and term infants (10, 22, 23). Notably, whereas Clark et al. (10) have showcased the presence of cardiorespiratory interaction in preterm infants and the fact that it increases with postnatal age, direct cardiac influence on respiration and respiratory influence on heart rate have not been disentangled. Overall, in this population, important questions regarding the physiological mechanisms of cardiorespiratory interactions remain unanswered.

In this study, we investigate cardiorespiratory coupling in preterm infants, incorporating the simultaneous analysis of HRV and respiration, as well as how they affect one another. We use KC as a safe and easily reproducible experimental setting to contrast changes in regulation during KC from periods in the incubator. We hypothesize that cardiorespiratory coupling is responsive to KC, i.e., increased comfort, and focus on uncovering the physiological mechanisms underpinning these changes, including the directionality of these mechanisms. We employ the signal processing algorithms of phase-rectified signal averaging (PRSA) and bivariate phase-rectified signal averaging (BPRSA) developed by Bauer et al. (4) and Schumann et al. (35). This approach enables the characterization of quasi-periodicities, which, for instance, may be distinctively associated with increases and decreases in heart rate (PRSA). Furthermore, any coupled respiratory phenomenon uniquely associated with increases and decreases in heart rate can be simultaneously characterized using BPRSA. Also, the analysis can be reversed to study, for example, changes in cardiac activity coupled to certain respiratory states such as peaks and troughs of respiration.

MATERIALS AND METHODS

Patient Population

Twenty stable preterm infants, 13 male and 7 female, born between 26 and 34 wk gestational age (GA) and admitted to the neonatal intensive care unit (NICU) of Máxima Medical Centre, Veldhoven, The Netherlands, between February and May 2017, were included in the study. Exclusion criteria were any serious clinical conditions at the time of inclusion (e.g., sepsis, necrotizing enterocolitis), conditions that interfered with breathing (mechanical ventilation), and severe brain pathology (intraventricular hemorrhage grade III/IV or cystic periventricular leukomalacia). Because the study was of an observational nature, the medical ethics committee provided a waiver (referred to as N16.101) in accordance with the Dutch law on medical research with humans. Table 1 characterizes the study participants; the median gestational age was 29.5 [interquartile range (IQR): 27.3–30.6] wk, with a birth weight of 1,192 (1,055–1,295) g. The postmenstrual age (gestational age + postnatal age) at the beginning of the study was 31 (29.9–32.4) wk. All infants contributed approximately five KC sessions over a period of ~8 days. This research was performed according to the principles of the Declaration of Helsinki.

Table 1. *Median and interquartile ranges (25th to 75th percentile) of patient characteristics at birth and during the study*

Characteristics	Median	25th Percentile	75th Percentile
Gestational age, wk	29.5	27.3	30.6
Birth weight, g	1,192	1,055	1,295
No. of KC sessions	5	4	6
Duration of KC sessions, min	90	75	107
PMA during the first KC session	31	29.9	32.4
Average PMA for all KC sessions	31	30.1	32.6
PNA during KC, days	10	6	15.8
Duration of data collection, days	8	7	8

KC, kangaroo care; PMA, postmenstrual age; PNA, postnatal age. PNA is the no. of days after birth. Duration of data collection is the no. of days from the 1st day of the study until the last day of the study.

Study Design

KC sessions were annotated by nurses based on recording the start (placement on parental chest) and end time (placement into the incubator) of KC. Multiple sessions of KC recorded from 20 infants accounted for intrapatient and interpatient variability, respectively, as described in our previous studies (17–19). Similarly to prior research, we excluded KC sessions <1 h and those without data for ≥ 1 h in the pre- and post-KC periods as well as those KC sessions where the pre- or post-KC period overlapped with the pre- or post-KC period of another KC session in the same infant. These criteria yielded 105 KC sessions for the final analysis. Representative 30-min epochs from the pre-, during-, and post-KC periods from each KC session, as described in a previous study, were used for all analysis (19).

Measurements: Vital Signs, Electrocardiography, and Chest Impedance

Routine patient monitoring, including the recording of vital signs, continued throughout the study. The patient monitor (Philips IntelliVue MX 800) processed the raw waveforms acquired via various sensors to provide measures of vital signs, including the heart rate [HR; using electrocardiography (ECG) at 250 Hz], the respiratory rate [using chest impedance (CI) at 62.5 Hz], the oxygen saturation (SpO_2; using pulse oximetry), and diaper temperature at a frequency of 1 Hz. The recordings of ECG and CI were synchronous since both were recorded from the same chest electrodes. All data were retrospectively retrieved from a data warehouse (PIIC iX, Data Warehouse Connect; Philips Medical Systems, Andover, MA).

Signal Preprocessing

A peak detection algorithm was used to detect the R-peaks in the ECG recordings (33), followed by calculating the interbeat intervals or R-R intervals (RRi). The time series of RRi, also known as the tachogram, reflected the HRV, which in turn can be characterized using different features.

Concerning the CI signal, the phasic flow of blood through the heart is known to generate artifacts in the CI corresponding to each heartbeat. These artifacts can mimic breathing since the phasic flow of blood creates a change in electrical impedance, similar to air flowing in and out of the lungs. Therefore, the CI was first filtered to remove all cardiac artifacts according to the method developed and tested by Lee et al. (21). Next, the CI was preprocessed by subtracting the mean value of the signal from itself, followed by normalization, entailing dividing the CI signal by the median of the absolute value of the signal. Unless specified, further references to the CI signal refer to this preprocessed signal with cardiac artifacts removed. Finally, the peaks and troughs of the CI signal corresponding to inhalation and exhalation were algorithmically detected.

Background on PRSA and BPRSA

Based on the work of Bauer et al. (4), we briefly describe the PRSA and BPRSA methods below. In subsequent sections, we describe how these methods were applied to preterm infants and detail the development of characteristic features for quantitatively interpreting the corresponding results.

PRSA is a signal analysis technique that is capable of detecting and quantifying quasi-periodic oscillations masked by the nonstationary nature of composite signals, artifacts, and noise (4). Notably, the presence of quasiperiodic oscillations is indicative of the underlying physiological regulatory processes. In adults, PRSA has been successfully applied to tachograms for predicting mortality after myocardial infarctions and has outperformed typical measures such as the left ventricular ejection fraction and other conventional measures of HRV (3).

PRSA can quantify the coherence time of each quasiperiodicity in the signal while the signal is in a certain phase. The phase is identified based on identifying anchor points (AP), which in their simplest form are merely the increasing and decreasing parts of the signal but may have more nuanced definitions, depending on the context of the application. The signals in the neighborhood around the APs are averaged to get a condensed, phase-rectified version of the original signal. This PRSA signal contains information on the physiological, possibly quasi-periodic mechanisms responsible for generating the corresponding APs. Since the PRSA technique synchronizes the phase of all (quasi)periodic components of the signal, irrespective of their frequencies or characteristic timescales, it integrates their contributions by accumulating the corresponding amplitudes at the center of the PRSA signal. By using different criteria for APs, PRSA can be used to separately analyze the quasi-periodicities associated with increasing and decreasing parts of the signal. APs are likely to lie on the steepest part of the ascent (or descent), especially for sinusoidal quasi-periodicities, since then the phase of underlying quasi-periodicity is closest to 0 (or π). For example, APs corresponding to an increase are defined as the set of i such that

$$\frac{1}{T}\sum_{j=0}^{T-1} x_{i+j} > \frac{1}{T}\sum_{j=1}^{T} x_{i-j} \qquad (1)$$

where x is the underlying signal such as the tachogram and T is freely changeable to select averages over a different number of points. For instance, to identify APs for all increases, $T = 1$. The parameter T also sets the upper frequency that can be detected using PRSA. Mathematically, it has been shown that PRSA is most sensitive to oscillations of frequency $f \approx 1/(2.5T)$ for signals containing nonstationarities (4). Thereby, increasing T has a low-pass filtering effect. Windows of the length $2L$ are defined around each AP and then averaged to yield the PRSA. APs close to the beginning or at the end of the time series, where no full surroundings of length $2L$ are available, are disregarded. This averaging procedure to generate the PRSA waveform, using data in the neighborhood of the APs, ensures that only those periodicities and quasi-periodicities that have a fixed phase relationship with the APs remain, whEREAS nonstationarities, artifacts, and noise get canceled out. Finally, *eq. 1* can yield APs corresponding to decreases if ">" is replaced with "<."

BPRSA and the Direction of Coupling

BPRSA is a generalization of the PRSA technique where APs are defined in one (trigger) signal while averaging is carried out in another (target) signal (2, 35). This approach enables the identification and study of coupling from the trigger to the target signal either because of direct interaction between them or via a tertiary mechanism that simultaneously affects both signals.

If anchor points a_i are defined by a *phenomenon A* in the selected trigger *signal A*, and the resulting average in target *signal B* shows *phenomenon B*, then we say that the system displays "coupling from *phenomenon A* to *phenomenon B*." Caution about interpretation is required. In particular, causality is not implied by this statement. It may be that *A* causes *B*, but there could be some other phenomenon, perhaps not seen in either signal, that causes both. Furthermore, the possibility that *B* causes *A* is not excluded.

If a system displays coupling from *A* to *B*, it may or may not show coupling from *B* to *A*. We see coupling from *A* to *B* if, when *A* occurs, *B* is sufficiently common that it survives the averaging over anchor points a_i. If we observe coupling from *A* to *B*, and we reverse the roles, so that *B* is the trigger signal and *A* is the target signal, at least some of the times that *B* occurs, *A* also occurs. However, some other phenomenon, *phenomenon C*, may occur in the *target signal A* so much more frequently that, upon averaging over the anchor points in *trigger signal B*, there is no visible coupling from *phenomenon B* to *phenomenon A*.

Since the direction of coupling is significant both observationally and physiologically, phrases like "*A* is coupled to *B*" or "coupling between *A* and *B*" are avoided, in favor of the exacting phrases "from *A* to *B*" or "from *B* to *A*." We use this language consistently below.

Parameter Selection and Feature Development for PRSA and BPRSA

For all pre-, during-, and post-KC periods, the PRSA waveforms corresponding to heart rate decelerations and heart rate accelerations were generated from the tachogram (from representative 30-min epochs of the pre-, during-, and post-KC periods) for parameter values of $t = 1$ and $t = 10$ with L = 150 RRi; $t = 1$ serves to uncover the underlying quasiperiodic mechanisms responsible for beat-to-beat changes in heart rate, whereas with $t = 10$, the quasiperiodic mechanisms for more sustained increases and decreases in heart rate can be obtained. For these PRSA waveforms, the following representative features were defined to characterize the waveform: *1*) the immediate deceleration response (IDR) and the immediate acceleration response (IAR) as the difference between the maximum and minimum values of RRi in the five data points after (including the AP) and before the AP, respectively, a feature that was aimed at capturing the maximal response of the heart rate in the immediate neighborhood of the AP; *2*) the slope of the deceleration response (SDR) and the slope of the acceleration response (SAR) as the slope of the line joining the maximum and minimum values of the RRi corresponding to the IDR and the IAR respectively, a feature that was aimed at capturing the rate of heart rate response; and *3*) the average deceleration response (ADR) and the average acceleration response (AAR) as the difference between the mean value of the 50 RRi after (including the AP) and the 50 RRi before the AP, a feature that was aimed at capturing the average heart rate response to the deceleration and acceleration, respectively.

Coupling from the heart to respiration. Using decelerations and accelerations in heart rate as triggers in the tachogram, we acquire the BPRSA waveform with $L = 2.4$ s (150 samples) in the respiration signal (target). It should be noted that the time corresponding to L is different for the tachogram and respiration signal but large enough to obtain the low frequencies of interest in both waveforms. The following features were used to characterize these BPRSA waveforms: *1*) the maximum respiratory amplitude (MRA) as the difference between the maximum and minimum amplitude of the respiratory oscillations, a feature that was aimed at capturing differences in the maximum tidal volumes as measured by CI amplitudes; *2*) the instantaneous slope at the anchor point (SAP), a feature that was aimed at identifying the phase of respiration at the AP (a negative value corresponds to the expiratory phase, whereas a positive value corresponds to the inspiratory phase); and *3*) the sample entropy (SampEn) of the respiratory oscillations (31), a feature that was used to quantify the regularity of BPRSA oscillations [a small value implies greater regularity, whereas a large value corresponds to the increased randomness of the oscillations; the SampEn was applied to 4.8 s ($2 \times L$) of the data with a run

length equal to 0.5 s, with a tolerance equal to 0.2 times the standard deviation of the BPRSA signal].

Throughout this work, before the PRSA and BPRSA waveforms acquired from the 105 sessions to yield the final representative PRSA and BPRSA waveforms of the pre-, during-, and post-KC periods were averaged, the mean values of the 105 constituent waveforms were subtracted from the corresponding waveforms (baseline subtraction), since we were interested in the effect of Kangaroo care rather than the absolute values per se. Therefore, both the PRSA and BPRSA waveforms, after baseline subtraction, oscillate about zero.

Coupling from respiration to heart. We also phase the respiratory signal (trigger), using as anchor points the location of inspiratory peaks and expiratory troughs, respectively (for $L = 2.4$ s, equivalent to 150 samples). Simultaneously, the BPRSA corresponding to the tachogram (target) was calculated ($L = 150$ RRi).

Frequency Analysis

Similar to traditional signal analysis where waveforms can be studied in both the time and frequency domains, the frequency spectrum of the PRSA and BPRSA waveforms can also be calculated. For all PRSA and BPRSA waveforms, the normalized power spectral density (PSD) was calculated. This method of calculating the PSD, based on rectified signals, has been proven to perform better than traditional spectral analysis of the original waveforms (2, 3). The frequency content of the PSD was measured in the time units of RRi^{-1} and s^{-1} (Hz) for RRi and respiration, respectively.

Respiratory Cessations

Preterm infants are susceptible to respiratory cessations that may, in turn, influence heart rate variability as well as cardiorespiratory coupling. Therefore, we employed the algorithm developed by Lee et al. (21) to identify respiratory cessations in the CI signal (with cardiac artifact removed). Next, we calculated the percentage of time that breathing ceased (summation of all cessations, irrespective of length) for the periods of pre-, during, and post-KC for all KC sessions. The duration of individual respiratory cessations that was considered valid was based on the rules provided by Lee et al (21). They ignored cessations <2 s and considered as valid all episodes when the infant ceased to breathe for a duration >5 s as well as episodes of <5 s if they were sufficiently close to other cessations (<3 s). We ignored cessations >120 s as potential artifacts.

Statistics

Where appropriate, statistical comparisons were performed using the two-sided Wilcoxon rank-sum test because data were expected to have a non-Gaussian distribution. All data were described using median (IQR) values. A nominal P value of ≤ 0.01 was considered statistically significant.

RESULTS

Representative 30-min epochs from each of the pre-, during-, and post-KC periods were used for all analysis. The vital signs corresponding to these periods are tabulated in Table 2. Heart rate and breathing rate decreased during KC by 3.5 beats/min and 3.7 breaths/min, respectively ($P < 0.01$) and returned to pre-KC levels during the post-KC period. SpO_2 and temperature were statistically comparable in all three periods.

Table 2. *Median values (IQR) of vital signs in the pre-KC, during-KC, and post-KC periods*

Vitals	Pre-KC	During KC	Post-KC
Heart rate, beats/min	155.9 (150.5–162.4)	152.5 (147.8–157.4)	154.2 (148–161.2)
Breathing rate, breaths/min	51.2 (42.8–58.9)	47.5 (39.5–56.3)	49.6 (42.1–56.9)
SpO_2, %	94.3 (92.4–96.6)	94.9 (92.4–96.8)	95.3 (92.3–97)
Temperature, °C	36.9 (36.6–37.1)	36.9 (36.6–37.1)	36.8 (36.5–37)

IQR, interquartile range; KC, kangaroo care; SpO_2, oxygen saturation.

PRSA of the Tachogram

By applying PRSA to heartbeats, i.e., with $t = 1$, we identified the presence of underlying (quasi)periodic signals that are phase synchronized to decelerations (Fig. 1*A1*) and accelerations (Fig. 1*C1*). Table 3 characterizes the PRSA waveforms corresponding to these decelerations and accelerations. The magnitude and rate of the immediate response to decelerations (IDR and SDR) and accelerations (IAR and SAR) remained statistically comparable in the pre-, during-, and post-KC periods. The average response to deceleration (ADR), on the other hand, decreased from the pre-KC to the during-KC period ($P < 0.01$) and remained comparable in the post-KC period. The average response to acceleration (AAR) was comparable across all periods. The magnitude of the average deceleration response was more than that of the average acceleration response (ADR $>$ AAR; Table 3), indicating fewer but more extensive decelerations, as opposed to accelerations. Notably, the coherence time (i.e., the time over which the phase, on average, is predictable) of the PRSA waveform and thereby that of the slowest quasi-periodicity appeared to be $\geq$25 RRi (Fig. 1, *A1* and *C1*). Note that most of the power is in the low-frequency range and is <0.05 RRi^{-1} (Fig. 1, *A2* and C2).

Coupling From the Heart to Respiration

The corresponding BPRSA waveforms (Fig. 1, *B* and *D*) show prominent oscillations, which by our definitions above constitute coupling from RRi to respiration, specifically from decelerations to respiration and from accelerations to respiration. We see in Fig. 1*B1* that upon averaging the respiration (target) signal over all anchor points in the tachogram (trigger) signal at which the heart rate is decreasing, there is coupling from decelerations to exhalation. Exhalation begins on average 0.3 to 0.5 s before the anchor point and ends on average <0.1 s after the anchor point. Similarly, Fig. 1*D1* shows coupling from heart rate accelerations to inhalation. (All the cautions mentioned earlier are relevant here. We may not conclude from this observation that decelerations cause exhalation or that accelerations cause inhalations. Indeed, it may be that inhalations sometimes cause accelerations or that a burst of sympathetic activity causes both.)

As seen in Fig. 1, the amplitude of these respiratory oscillations (average of 105 sessions) increases during KC and post-KC compared with the pre-KC period. The presence of regularity in the respiratory oscillations (BPRSA) was confirmed by low values of SampEn (Table 3). Because in the during- and the post-KC periods the amplitude of the averaged BPRSA waveform was larger, despite no increase in the regularity or maximal respiratory amplitude (MRA) of the constituent respiratory waveforms (which in fact decreases during KC), we can deduce that there was increased constructive interference (as in wave interference in classical physics)

Table 3. *Median (IQR) of characteristics of cardiorespiratory coupling in the pre-KC, during-KC and post-KC period (t = 1)*

Figure	Pre-KC	During-KC	Post-KC	*P Value 1*	*P Value 2*	*P Value 3*
Figure 1*A*						
IDR, ms	5.89 (4.53–9.47)	5.36 (4.16–9.28)	5.76 (4.39–8.52)	0.13	0.41	0.38
SDR, ms/RRi	5.10 (3.62–9.04)	4.78 (3.54–3.38)	4.79 (3.70–7.61)	0.40	0.92	0.37
ADR, ms/RRi	1.59 (0.95–2.21)	1.09 (0.66–1.77)	1.28 (0.67–2.15)	0.001*	0.13	0.08
Figure 1*B*						
MRA	0.30 (0.19–0.44)	0.24 (0.14–0.37)	0.32 (0.19–0.44)	0.003*	0.01*	0.63
SAP ($\times 10^{\wedge -2}$)	−0.19 (−1.27–0.91)	−0.21 (−0.97–0.42)	−0.41 (−0.97–0.42)	0.80	0.83	0.75
SampEn	0.022 (0.016–0.030)	0.024 (0.015–0.032)	0.022 (0.015–0.029)	0.60	0.48	0.80
Figure 1*C*						
IAR (ms)	5.24 (4.19–9.14)	4.84 (3.91–8.22)	5.25 (4.22–7.68)	0.15	0.43	0.45
SAR (ms/RRi)	−4.73 (−8.72–−3.63)	−4.33 (−7.82–−3.37)	−4.50 (−6.84–−3.53)	0.16	0.64	0.31
AAR (ms/RRi)	1.36 (0.80–1.92)	1.17 (0.70–1.66)	1.11 (0.64–1.67)	0.20	0.76	0.12
Figure 1*D*						
MRA	0.29 (0.19–0.43)	0.23 (0.13–0.37)	0.30 (0.17–0.43)	0.004*	0.02	0.69
SAP ($\times 10^{\wedge -2}$)	0.22 (−0.84–1.21)	0.30 (−0.25–1.0)	0.34 (−0.35–1.21)	0.41	0.97	0.52
SampEn	0.025 (0.018–0.034)	0.022 (0.015–0.031)	0.022 (0.014–0.029)	0.07	0.74	0.03

AAR, average acceleration response; ADR, average deceleration response; IAR, immediate acceleration response; IDR, immediate deceleration response; KC, kangaroo care; MRA, maximum respiratory amplitude; RRi, R-R interval; SDR, slope of the deceleration response; SampEn, sample entropy; SAP, slope at the anchor point; SAR, slope of the acceleration response. *P value 1* corresponds to the comparison of the pre-KC and during-KC periods, *P value 2* corresponds to the comparison of the during-KC and the post-KC periods, and *P value 3* corresponds to the comparison of the pre-KC and the post-KC periods. *$P < 0.01$.

during KC and post-KC. The instantaneous slope of the respiration signal at the anchor point in the tachogram (SAP) confirms the visual observations of Fig. 1, with coupling from decelerations to negative SAP (expiration) and from accelerations to positive SAP (inspiration). The corresponding PSD shows that the majority of the power is centered between 0.5 and 1.5 Hz and that there also exists a small peak ~0.10–0.20 Hz. Furthermore, notably, the BPRSA waveforms corresponding to decelerations and accelerations are practically the inverse of one another.

Figure 2 shows the results of the same analysis as in Fig. 1, but with $t = 10$. The coherence time of the PRSA signal can be seen to increase. Compared with the pre-KC period, the immediate deceleration and acceleration response (IDR and IAR) were lower during KC, as was the rate of response (Table 4). During the post-KC period, the response was similar to that seen in the pre-KC period. About the average deceleration (ADR) and acceleration response (AAR) were reduced during KC and remained low in the post-KC period as well ($P < 0.01$). Compared with Fig. 1, the corresponding PSD of the PRSA waveforms indicates an increase in power in the low-frequency band. The PSD of the BPRSA waveforms show only low-frequency oscillations; compared with the BPRSA waveforms of Fig. 1, effects around the respiratory frequency of 1 Hz have disappeared entirely.

PRSA of Respiration.

Figure 3 shows the phase-rectified waveforms of the respiration signal, which were rectified based on the location of inspiratory peaks and expiratory troughs. These waveforms are the inverse of each other and have a PSD that peaks between 0.5 and 1.5 Hz. Notably, there was no peak ~0.10–0.20 Hz.

Coupling From Respiration to Heart

The corresponding BPRSA from the respiration signal to the tachogram, again using as anchor points the peaks and troughs of inspiration and expiration, respectively, showed a decrease in heart rate near both sets of anchor points. The power in the PSD corresponding to the BPRSA waveform was largely restricted to low frequency (<0.01 RRi^{-1}).

With regard to respiratory cessations, the total period that infants were not breathing was comparable in the pre-, during-, and post-KC periods at ~10%. Figure 4 shows the boxplots corresponding to the total duration of cessation, which was measured as a percentage of total time. Based on histogram analysis (data not shown), the typical duration of cessations was comparable as well.

DISCUSSION

In this explorative study in preterm infants, we analyzed the cardiac and respiratory regulatory mechanisms as well as the coupling between them. In particular, we analyzed the coupling from fluctuations in the heart rate to respiratory oscillations and vice versa. Furthermore, we stratified these oscillations based on the dynamics of the signal, i.e., decelerations and accelerations in the heart rate and inspiration and expiration during respiration. We contrasted changes in autonomic regulation during KC with periods in the incubator and hypothesized that cardiorespiratory coupling is responsive to KC.

By using PRSA on cardiac activity, stratified by decelerations and accelerations, we demonstrated that the physiological mechanisms for decelerations and accelerations were not the converse of one another. For instance, both the deceleration- and acceleration-related modulation, as reflected by the features ADR and AAR, showed a reduction during KC as opposed to the pre-KC period, but throughout, the absolute value of the ADR was higher than the AAR, indicating that the number of accelerations exceeded the number of decelerations. This finding points to the presence of an unstable regulatory control mechanism prone to overshooting (severe decelerations) that requires multiple accelerations to maintain a stable heart rate. KC appears to improve cardiac regulation by reducing the severity of heart rate decelerations, with the ratio of the number of decelerations to the number of accelerations becoming closer to unity. These results reaffirm previous findings, which identified that infants are routinely prone to physiolog-

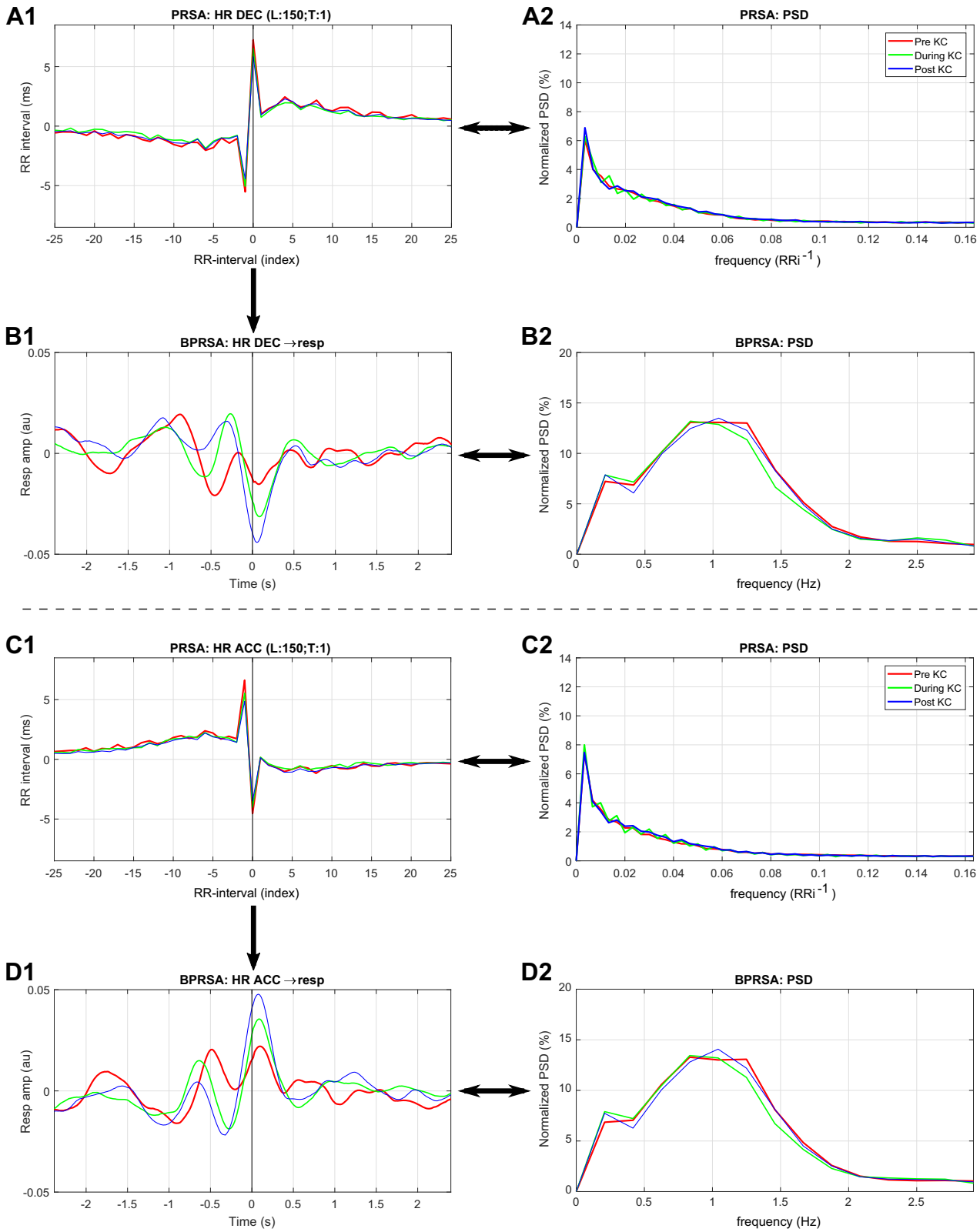

Fig. 1. *Left*: phase-rectified signal averaging (PRSA; *A1*, *A2*, *C1*, and *C2*) and bivariate phase-rectified signal averaging (BPRSA; *B1*, *B2*, *D1*, and *D2*) of the tachograms and the corresponding respiratory signals coupled to decelerations (above the dashed line) and accelerations (below the dashed line) for $t = 1$. Downward arrows indicate the coupling between the PRSA and the BPRSA waveforms. *Right*: power spectral density (PSD) of the corresponding phase-rectified signals, whereas the horizontal bidirectional arrows show the equivalence of the time and frequency domains. Note that the *x*-axes of both the PRSA and BPRSA signals are centered at 0 (black vertical line) but have different time units. Correspondingly, the *x*-axes for the PSD of the tachograms is in units of R-R intervals $(\text{RRi})^{-1}$, whereas that of respiration is in Hz.

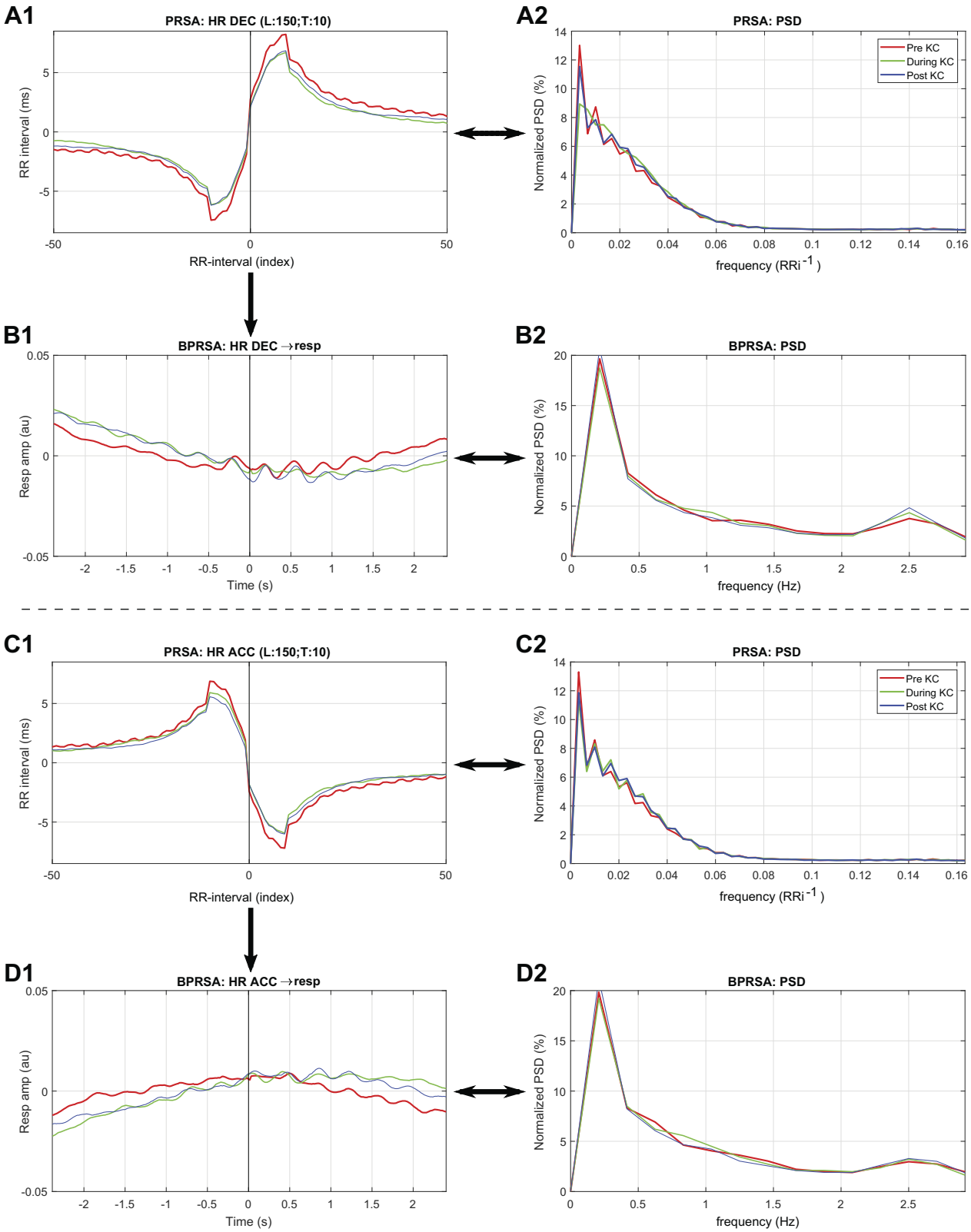

Fig. 2. *Left*: phase-rectified signal averaging (PRSA; *A1*, *A2*, *C1*, and *C2*) and bivariate phase-rectified signal averaging (BPRSA; *B1*, *B2*, *D1*, and *D2*) of the tachograms and the corresponding respiratory signals coupled to decelerations (above the dashed line) and accelerations (below the dashed line) for $t = 10$. Downward arrows indicate the coupling between the PRSA and the BPRSA waveforms. *Right*: power spectral density (PSD) of the corresponding phase-rectified signals, whereas the horizontal bidirectional arrows show the equivalence of the time and frequency domains. Note that the *x*-axes of the PRSA and BPRSA signals are both centered at 0 (black vertical line) but have different time units. Correspondingly, the *x*-axes for the PSD of the tachograms is in units of R-R intervals $(\text{RRi})^{-1}$, whereas that of respiration is in Hz.

Table 4. *Median (IQR) of characteristics of cardiorespiratory coupling in the pre-KC, during-KC, and post-KC periods (t = 10)*

Figure	Pre-KC	During-KC	Post-KC	*P Value 1*	*P Value 2*	*P Value 3*
Figure 2*A*						
IDR, ms	10.55 (6.94–14.72)	8.52 (6.00–11.12)	9.21 (7.01–11.95)	0.001*	0.11	0.09
SDR, ms/RRi	1.21 (0.78–1.71)	0.97 (0.66–1.23)	1.02 (0.77–1.32)	0.001*	0.14	0.06
ADR, ms/RRi	6.06 (4.34–7.62)	4.38 (3.14–5.78)	4.79 (3.96–6.39)	<0.0001*	0.02	0.002*
Figure 2*B*						
MRA	0.09 (0.05–0.12)	0.08 (0.05–0.11)	0.09 (0.09–0.13)	0.23	0.05	0.55
SAP ($\times 10^{-2}$)	−0.03 (−0.24–0.18)	0.03 (−0.13–0.23)	0.01 (−0.26 to 0.17)	0.02	0.04	0.87
SampEn	0.023 (0.017–0.035)	0.021 (0.014–0.036)	0.024 (0.017–0.035)	0.19	0.22	0.93
Figure 2*C*						
IAR, ms	9.15 (6.11–13.32)	7.48 (5.64–10.09)	8.06 (6.34–10.93)	0.01	0.24	0.15
SAR, ms/RRi	−1.04 (−1.5 to −0.67)	−0.85 (−1.13 to −0.62)	−0.89 (−1.21 to −0.70)	0.008*	0.27	0.12
AAR, ms/RRi	5.35 (3.97–6.98)	4.12 (3.02–5.43)	4.42 (3.67–5.58)	<0.0001*	0.14	0.001*
Figure 2*D*						
MRA	0.07 (0.05–0.11)	0.07 (0.05–0.10)	0.07 (0.05–0.12)	0.23	0.12	0.90
SAP ($\times 10^{-2}$)	−0.03 (−0.19 to 0.13)	0.05 (−0.08–0.22)	0.06 (−0.08 to 0.17)	0.003*	0.53	0.02
SampEn	0.025 (0.016–0.043)	0.025 (0.018–0.040)	0.022 (0.014–0.033)	0.99	0.06	0.07

AAR, average acceleration response; ADR, average deceleration response; IAR, immediate acceleration response; IDR, immediate deceleration response; IQR, interquartile range; KC, kangaroo care; MRA, maximum respiratory amplitude; SampEn, sample entropy; SAP, slope at the anchor point; SAR, slope of the acceleration response; SDR, slope of the deceleration response. *P value 1* corresponds to the comparison of the pre-KC and the during-KC periods, *P value 2* corresponds to the comparison of the during-KC and the post-KC periods, and *P value 3* corresponds to the comparison of the pre-KC and the post-KC periods. *$P < 0.01$.

ically undesirable heart rate decelerations, the severity of which decreases during KC (19).

Because phase rectification shows the overall capacity for deceleration and acceleration without necessarily being linked to a single physiological process, frequency analysis was used to identify the contributions of the underlying physiological mechanisms. The PSD of the PRSA waveforms corresponding to decelerations and accelerations as shown in Figs. 1 and 2 indicates that the physiological mechanisms responsible for the same occurred at frequencies <0.05 RRi^{-1} ($\approx$0.016–0.025 Hz, assuming a heart rate between 120 and 180 beats/min). Therefore, these effects may be attributable to mechanisms such as neurohormonal influences or peristaltic movements ($<$ 0.04 Hz) (20, 25, 29, 38).

Coupling From the Heart to Respiration

Figures 1 and 2 clearly show couplings from decelerations and accelerations in the heart rate to respiratory oscillations. These coupled respiratory oscillations should not be confused with the phenomenon of RSA found in adults, which is defined as coupling from respiration to heart rate, inhalation to acceleration, and exhalation to deceleration (38). The presence of these respiratory oscillations is notable since in the absence of an interrelationship between the trigger (changes in heart rate) and the target (respiratory signal) the corresponding BPRSA waveform would have been a flat line.

In this study, we identified that the BPRSA waveforms (of respiratory oscillations) coupled to decelerations and accelerations were the inverse of one another, suggesting a linear response mechanism of the underlying physiological system(s). We can also observe that for the beat-to-beat decelerations and accelerations, respectively (PRSA with $t = 1$), there occurred an expiratory and inspiratory peak, on average, with a latency of $\sim$0.06–0.09 s. The identification of this latency is in agreement with previous findings on cardiorespiratory coupling in preterm infants (10, 12). The PSD of the BPRSA waveform showed a broad peak at $\sim$1 Hz, matching the respiratory frequency. A smaller peak can be seen at $\sim$0.10–0.20 Hz, which is possibly related to baroreflex activity modulating the respiratory pattern following changes in heart rate (24, 39).

Upon analyzing more sustained decelerations and accelerations (PRSA with $t = 10$; Fig. 2), a decrease and increase in the corresponding respiratory amplitude is present, but only at low frequency (0.10–0.20 Hz). Together, these BPRSA results suggest the presence of a higher frequency coupling occurring from beat to beat and breath to breath, whereas a lower frequency coupling potentially modulated by the baroreflex persists throughout. The presence of coupling, overriding the natural tendency of systems to work independently of one another (37), suggests a physiological benefit brought about by it. The fact that the coupling appears to be more pronounced during and after KC, as evident by the increased amplitude of respiratory oscillations coupled to decelerations and accelerations of heart rate (BPRSA waveforms; Fig. 1), supports this. Along similar lines, increased postmenstrual age and quiet sleep have also been reported to increase cardiorespiratory coupling (10, 12, 22, 23).

Coupling From Respiration to Heart

In Fig. 3, we show the coupling from peaks of inspiration and troughs of expiration to cardiac activity. Unsurprisingly, the corresponding PSD of the PRSA is broad and centered at $\sim$1 Hz, i.e., the typical frequency of respiration (see Table 2). Remarkably, we do not observe coupling from peaks of inspiration to the acceleration of heart rate. Thus we do not observe the phenomenon of RSA. Rather, the coupled cardiac response to both peaks and troughs of respiration is a small (2–3 ms) and gradual deceleration of the heart rate.

Furthermore, if instead of the peaks and troughs of inspiration and expiration the midpoints of inspiration and expiration were used for rectification, the coupled cardiac response was still a gradual deceleration of the heart rate but of lower amplitude (data not shown) than that seen upon using the peaks

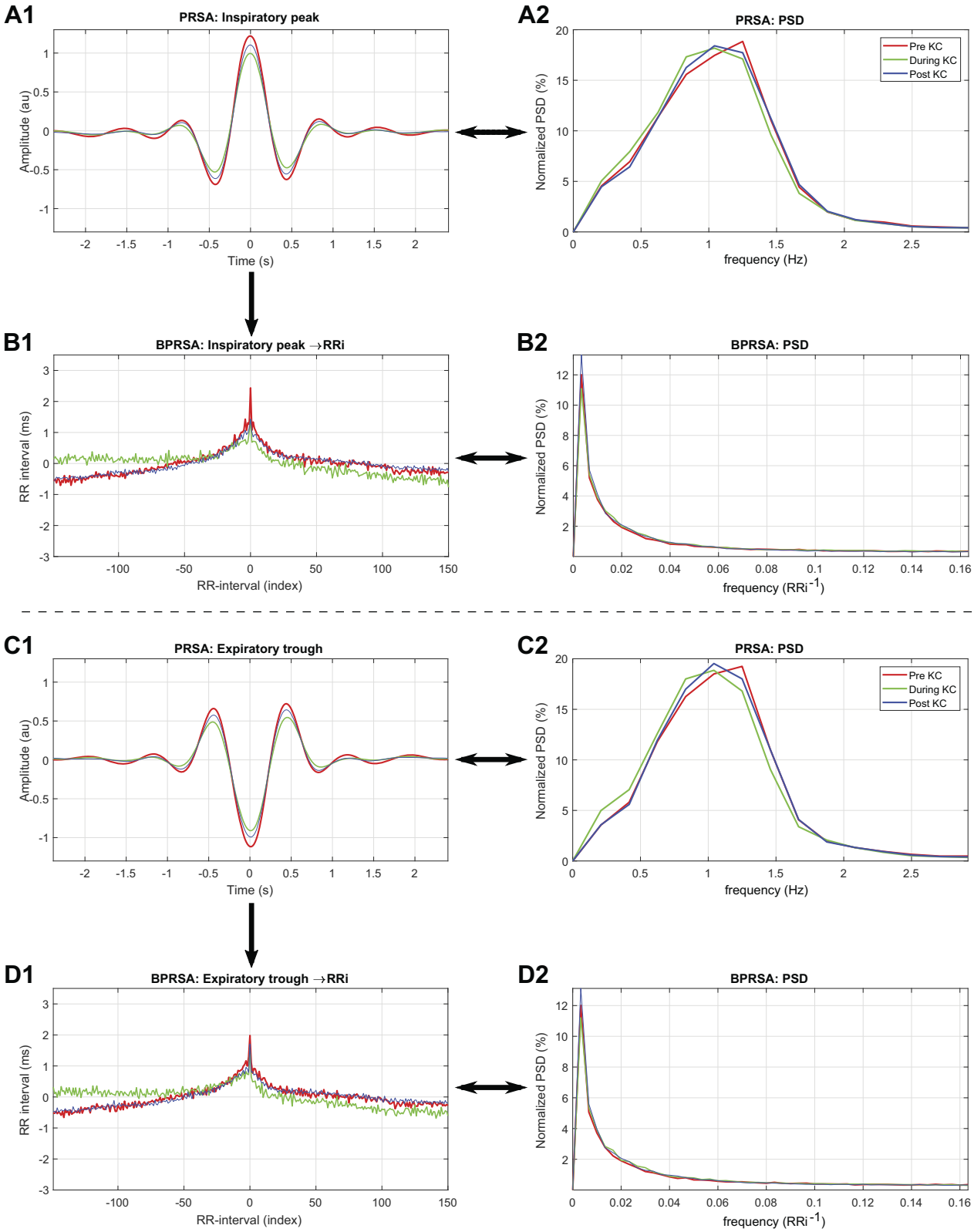

Fig. 3. *Left*: phase-rectified signal averaging (PRSA; *A1*, *A2*, *C1*, and *C2*) of the respiratory signals coupled to inspiratory peaks (above the dashed line) and expiratory troughs (below the dashed line) along with the bivariate phase-rectified signal averaging (BPRSA) of the corresponding tachograms (*B1*, *B2*, *D1*, and *D2*). Vertical downward arrows indicate the coupling between the PRSA and the BPRSA waveforms. *Right*: power spectral density (PSD) of the corresponding phase-rectified signals, whereas the horizontal bidirectional arrows show the equivalence of the time and frequency domains.

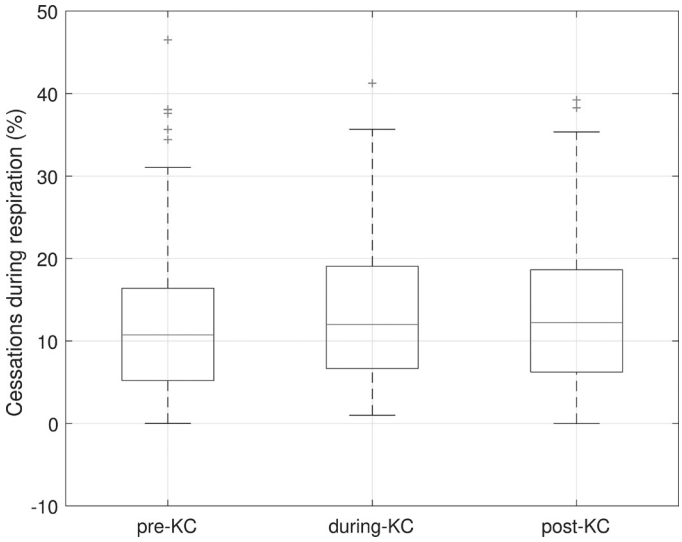

Fig. 4. %Total time that respiration ceased in the study population corresponding to the pre-, during-, and post-kangaroo care (KC) periods represented as boxplots, with each KC session contributing 1 data point. All cessations were added to calculate the total time corresponding to cessations. Statistically, there were no differences among the 3 periods.

and troughs of inspiration and expiration, respectively. Additionally, the BPRSA waveform was flat if the rectification of the respiratory waveform was based on the entire duration of inspiration or expiration (data not shown). Together, these findings suggest that it is the mechanical effect of maximal inspiration and expiration that triggers the decelerative cardiac response. Note that our findings do not suggest that all inspirations and expirations were associated with these decelerations in heart rate. Possibly it arises only in conjunction with, for instance, periodic breathing, other forms of breath amplitude modulation, or periodic peristaltic movements, since the corresponding PSD peaks at low frequency alone approximately once every 6–7 min. These findings may also explain the results by Clark et al. (10), where respiratory influences on RRi were present for only $<$20% of the total time (3.3 of 18 patient yr) analyzed.

As in our study, there are also other reports that that do not observe RSA in preterm infants (10, 30). In adults, RSA is reported to be caused by vagal influences on the heart during expiration, which ceases during inspiration, whereas in contrast sympathetic motor neurons are excited during inspiration and appear mildly inhibited during expiration (5). The degree of heart rate modulation appears to be a function of respiratory period and depth (26). We speculate that in preterm infants the differences in respiratory period and depth are insufficient in generating sinus arrhythmia. These findings become more important considering that, concerning cessations in breathing, a potential sign of insufficient vagal suppression, there were no statistically significant differences between the pre-, during-, and post-KC periods.

Overall, based on the bidirectional analysis of the cardiac and respiratory systems using the BPRSA method, we observed coupling from heart rate decelerations and accelerations to expiration and inspiration, respectively, whereas in the other direction we observed coupling from both peaks and troughs of respiration to small decelerations of the heart rate. This nonsymmetric coupling suggests that there are two distinct branches of cardiorespiratory coupling that modulate HRV in preterm infants, evidence of which has also been illustrated elsewhere (14). Our work offers new, differentiated insights into this bidirectional interaction.

Furthermore, we assessed mechanisms involved in the integrated control of cardiac and respiratory systems in response to the experimental condition of KC. Other studies have used, for instance, sleep state as a window into autonomic regulation (40). In contrast, KC is longer-lasting, enabling the analysis of lower-frequency components of physiological systems as well as enabling the study of autonomic regulation during a state and not in response to a state change. Therefore, our research contributes to an improved understanding of physiology and cardiorespiratory coupling in preterm infants, offering opportunities for improving therapeutic practices as well as for evaluating new interventions by studying changes in cardiorespiratory coupling, the precedence for which using HRV has already been set elsewhere (17, 18).

Some limitations of the study need to be accounted for. Although both the cardiac and respiratory systems are potentially influenced by posture, we did not correct for differences in posture during KC versus pre- and post-KC. During KC, infants are prone, whereas in the incubator infants are typically either prone or in the lateral position (16). Furthermore, since this study was of a within-subject design, the postmenstrual age was not a confounding factor. However, quiet sleep may have been a confounding factor, since this is known to increase during KC, potentially contributing to enhanced cardiorespiratory coupling (22). Unfortunately, information on the distribution of sleep states was unavailable. Additionally, we did not correct for methods of respiratory support; most infants, as is common in a preterm NICU population, were on nasal continuous positive airway pressure ventilation. However, infants on mechanical ventilation (intubated infants) were specifically excluded. We included only a homogeneous group of clinically stable preterm infants, limiting the generalizability of our findings outside a comparable population. Therefore, in future work, we will extend our analysis to study, for instance, the maturational trajectory of infants. Other possibilities for future analysis include studying the cardiorespiratory coupling between a parent and their infant during KC.

Conclusions

In this study of preterm infants, we selectively analyzed coupling from accelerations and decelerations in heart rate to respiratory oscillations and coupling from peaks and troughs of respiration to changes in heart rate using the BPRSA method. Preterm infants do exhibit cardiorespiratory coupling, and this coupling is nonsymmetric with regard to the direction of coupling. Upon examining coupling from heart rate to respiration, using the tachogram as the trigger signal and points of heart rate acceleration or deceleration as anchor points, the resulting average respiration signal showed inhalation or exhalation, respectively. On the other hand, examining coupling from respiration to heart rate, using either peaks or troughs of respiration signal as the trigger points, the averaged tachogram showed marginal decelerations in the heart rate. KC, which is considered to be a comfortable and therapeutic intervention,

served as an experimental setting to contrast changes in regulation during KC versus periods in the incubator.

ACKNOWLEDGMENTS

This research was performed in the framework of Eindhoven MedTech Innovation Center.

DISCLOSURES

No conflicts of interest, financial or otherwise, are declared by the authors.

AUTHOR CONTRIBUTIONS

R.J., S.V.H., and C.v.P. analyzed data; R.J., D.K., X.L., L.F., S.V.H., C.v.P., and P.A. interpreted results of experiments; R.J. and D.K. prepared figures; R.J., D.K., S.V.H., and P.A. drafted manuscript; R.J., D.K., X.L., L.F., S.V.H., C.v.P., and P.A. edited and revised manuscript; R.J., D.K., X.L., L.F., S.V.H., C.v.P., and P.A. approved final version of manuscript; D.K. performed experiments.

REFERENCES

1. **Banihashemi L, Rinaman L.** Repeated brief postnatal maternal separation enhances hypothalamic gastric autonomic circuits in juvenile rats. *Neuroscience* 165: 265–277, 2010. doi:10.1016/j.neuroscience.2009.09.081.
2. **Bauer A, Barthel P, Müller A, Kantelhardt J, Schmidt G.** Bivariate phase-rectified signal averaging--a novel technique for cross-correlation analysis in noisy nonstationary signals. *J Electrocardiol* 42: 602–606, 2009. doi:10.1016/j.jelectrocard.2009.06.023.
3. **Bauer A, Kantelhardt JW, Barthel P, Schneider R, Mäkikallio T, Ulm K, Hnatkova K, Schömig A, Huikuri H, Bunde A, Malik M, Schmidt G.** Deceleration capacity of heart rate as a predictor of mortality after myocardial infarction: cohort study. *Lancet* 367: 1674–1681, 2006. doi:10.1016/S0140-6736(06)68735-7.
4. **Bauer A, Kantelhardt JW, Bunde A, Barthel P, Schneider R, Malik M, Schmidt G.** Phase-rectified signal averaging detects quasi-periodicities in non-stationary data. *Physica A* 364: 423–434, 2006. doi:10.1016/j.physa.2005.08.080.
5. **Berntson GG, Cacioppo JT, Quigley KS.** Respiratory sinus arrhythmia: autonomic origins, physiological mechanisms, and psychophysiological implications. *Psychophysiology* 30: 183–196, 1993. doi:10.1111/j.1469-8986.1993.tb01731.x.
6. **Blencowe H, Cousens S, Chou D, Oestergaard M, Say L, Moller A-B, Kinney M, Lawn J; Born Too Soon Preterm Birth Action Group.** Born too soon: the global epidemiology of 15 million preterm births. *Reprod Health* 10, *Suppl* 1: S2, 2013. doi:10.1186/1742-4755-10-S1-S2.
7. **Bloch-Salisbury E, Zuzarte I, Indic P, Bednarek F, Paydarfar D.** Kangaroo care: cardio-respiratory relationships between the infant and caregiver. *Early Hum Dev* 90: 843–850, 2014. doi:10.1016/j.earlhumdev.2014.08.015.
8. **Charpak N, Ruiz JG, Zupan J, Cattaneo A, Figueroa Z, Tessier R, Cristo M, Anderson G, Ludington S, Mendoza S, Mokhachane M, Worku B.** Kangaroo mother care: 25 years after. *Acta Paediatr* 94: 514–522, 2005. doi:10.1080/08035250510027381.
9. **Chatow U, Davidson S, Reichman BL, Akselrod S.** Development and maturation of the autonomic nervous system in premature and full-term infants using spectral analysis of heart rate fluctuations. *Pediatr Res* 37: 294–302, 1995. doi:10.1203/00006450-199503000-00008.
10. **Clark MT, Rusin CG, Hudson JL, Lee H, Delos JB, Guin LE, Vergales BD, Paget-Brown A, Kattwinkel J, Lake DE, Moorman JR.** Breath-by-breath analysis of cardiorespiratory interaction for quantifying developmental maturity in premature infants. *J Appl Physiol (1985)* 112: 859–867, 2012. doi:10.1152/japplphysiol.01152.2011.
11. **Conde-Agudelo A, Díaz-Rossello JL.** Kangaroo mother care to reduce morbidity and mortality in low birthweight infants. *Cochrane Database Syst Rev* 4: CD002771, 2014. [Update in: *Cochrane Database Syst Rev* (8) CD002771, 2016. 10.1002/14651858.CD002771.pub4] doi:10.1002/14651858.CD002771.pub3.
12. **Elder DE, Larsen PD, Galletly DC, Campbell AJ.** Cardioventilatory coupling in preterm and term infants: effect of position and sleep state. *Respir Physiol Neurobiol* 174: 128–134, 2010. doi:10.1016/j.resp.2010.05.012.
14. **Indic P, Bloch-Salisbury E, Bednarek F, Brown EN, Paydarfar D, Barbieri R.** Assessment of cardio-respiratory interactions in preterm infants by bivariate autoregressive modeling and surrogate data analysis. *Early Hum Dev* 87: 477–487, 2011. doi:10.1016/j.earlhumdev.2011.04.001.
15. **Johnston CC, Stevens B, Pinelli J, Gibbins S, Filion F, Jack A, Steele S, Boyer K, Veilleux A.** Kangaroo care is effective in diminishing pain response in preterm neonates. *Arch Pediatr Adolesc Med* 157: 1084–1088, 2003. doi:10.1001/archpedi.157.11.1084.
16. **Joshi R, van Pul C, Sanders A, Weda H, Bikker JW, Feijs L, Andriessen P.** A strategy to reduce critical cardiorespiratory alarms due to intermittent enteral feeding of preterm neonates in intensive care. *Interact J Med Res* 6: e20, 2017. doi:10.2196/ijmr.7756.
17. **Kommers D, Joshi R, Pul CV, Feijs L, Oei G, Oetomo SB, Andriessen P.** Unlike kangaroo care, mechanically simulated Kangaroo care does not change heart rate variability in preterm neonates. *Early Hum Dev* 121: 27–32, 2018. doi:10.1016/j.earlhumdev.2018.04.031.
18. **Kommers DR, Joshi R, van Pul C, Feijs L, Bambang Oetomo S, Andriessen P.** Changes in autonomic regulation due to kangaroo care remain unaffected by using a swaddling device. *Acta Paediatr*. In press. doi:10.1111/apa.14484.
19. **Kommers DR, Joshi R, van Pul C, Atallah L, Feijs L, Oei G, Bambang Oetomo S, Andriessen P.** Features of heart rate variability capture regulatory changes during kangaroo care in preterm infants. *J Pediatr* 182: 92–98.e1, 2017. doi:10.1016/j.jpeds.2016.11.059.
20. **Larsen PD, Galletly DC.** Cardioventilatory coupling in heart rate variability: the value of standard analytical techniques. *Br J Anaesth* 87: 819–826, 2001. doi:10.1093/bja/87.6.819.
21. **Lee H, Rusin CG, Lake DE, Clark MT, Guin L, Smoot TJ, Paget-Brown AO, Vergales BD, Kattwinkel J, Moorman JR, Delos JB.** A new algorithm for detecting central apnea in neonates. *Physiol Meas* 33: 1–17, 2012. doi:10.1088/0967-3334/33/1/1.
22. **Lucchini M, Pini N, Fifer WP, Burtchen N, Signorini MG.** Entropy information of cardiorespiratory dynamics in Neonates during sleep. *Entropy (Basel)* 19: 225, 2017. doi:10.3390/e19050225.
23. **Lucchini M, Pini N, Fifer WP, Burtchen N, Signorini MG.** Characterization of cardiorespiratory phase synchronization and directionality in late premature and full term infants. *Physiol Meas* 39: 064001, 2018. doi:10.1088/1361-6579/aac553.
24. **Mazursky JE, Birkett CL, Bedell KA, Ben-Haim SA, Segar JL.** Development of baroreflex influences on heart rate variability in preterm infants. *Early Hum Dev* 53: 37–52, 1998. doi:10.1016/S0378-3782(98)00038-3.
25. **Omari TI, Benninga MA, Barnett CP, Haslam RR, Davidson GP, Dent J.** Characterization of esophageal body and lower esophageal sphincter motor function in the very premature neonate. *J Pediatr* 135: 517–521, 1999. doi:10.1016/S0022-3476(99)70178-2.
26. **Overbeek TJM, van Boxtel A, Westerink JHDM.** Respiratory sinus arrhythmia responses to cognitive tasks: effects of task factors and RSA indices. *Biol Psychol* 99: 1–14, 2014. doi:10.1016/j.biopsycho.2014.02.006.
27. **Park MK.** *Pediatric Cardiology for Practitioners* (6th ed.). St. Louis, MO: Mosby, 2014.
28. **Rajendra Acharya U, Paul Joseph K, Kannathal N, Lim CM, Suri JS.** Heart rate variability: a review. *Med Biol Eng Comput* 44: 1031–1051, 2006. doi:10.1007/s11517-006-0119-0.
29. **van Ravenswaaij-Arts CM, Kollée LA, Hopman JC, Stoelinga GB, van Geijn HP.** Heart rate variability. *Ann Intern Med* 118: 436–447, 1993. doi:10.7326/0003-4819-118-6-199303150-00008.
30. **Reulecke S, Schulz S, Voss A.** Autonomic regulation during quiet and active sleep states in very preterm neonates. *Front Physiol* 3: 61, 2012. doi:10.3389/fphys.2012.00061.
31. **Richman JS, Moorman JR.** Physiological time-series analysis using approximate entropy and sample entropy. *Am J Physiol Heart Circ Physiol* 278: H2039–H2049, 2000. doi:10.1152/ajpheart.2000.278.6.H2039.
32. **De Rogalski Landrot I, Roche F, Pichot V, Teyssier G, Gaspoz JM, Barthelemy JC, Patural H.** Autonomic nervous system activity in premature and full-term infants from theoretical term to 7 years. *Auton Neurosci* 136: 105–109, 2007. doi:10.1016/j.autneu.2007.04.008.
33. **Rooijakkers MJ, Rabotti C, Oei SG, Mischi M.** Low-complexity R-peak detection for ambulatory fetal monitoring. *Physiol Meas* 33: 1135–1150, 2012. doi:10.1088/0967-3334/33/7/1135.
34. **Sahar T, Shalev AY, Porges SW.** Vagal modulation of responses to mental challenge in posttraumatic stress disorder. *Biol Psychiatry* 49: 637–643, 2001. doi:10.1016/S0006-3223(00)01045-3.

35. **Schumann AY, Kantelhardt JW, Bauer A, Schmidt G.** Bivariate phase-rectified signal averaging. *Physica A* 387: 5091–5100, 2008. doi:10.1016/j.physa.2008.05.002.
36. **Sobiech T, Buchner T, Krzesiński P, Gielerak G.** Cardiorespiratory coupling in young healthy subjects. *Physiol Meas* 38: 2186–2202, 2017. doi:10.1088/1361-6579/aa9693.
37. **Soize C, Ghanem R.** Physical Systems with Random Uncertainties: Chaos Representations with Arbitrary Probability Measure. *SIAM J Sci Comput* 26: 395–410, 2004. doi:10.1137/S1064827503424505.
38. **Malik M, Bigger JT, Camm AJ, Kleiger RE, Malliani A, Moss AJ, Schwartz PJ; Task Force of the European Society of Cardiology and the North American Society of Pacing and Electrophysiology.** Heart rate variability. Standards of measurement, physiological interpretation, and clinical use. *Eur Heart J* 17: 354–381, 1996. doi:10.1093/oxfordjournals.eurheartj.a014868.
39. **Tzeng YC, Larsen PD, Galletly DC.** Mechanism of cardioventilatory coupling: insights from cardiac pacing, vagotomy, and sinoaortic denervation in the anesthetized rat. *Am J Physiol Heart Circ Physiol* 292: H1967–H1977, 2007. doi:10.1152/ajpheart.01049.2006.
40. **Yiallourou SR, Wallace EM, Whatley C, Odoi A, Hollis S, Weichard AJ, Muthusamy JS, Varma S, Cameron J, Narayan O, Horne RSC.** Sleep: A window into autonomic control in children born preterm and growth restricted. *Sleep (Basel)* 40: 5, 2017. doi:10.1093/sleep/zsx048.